Stochastic Analysis of the Variability of Groundwater Flow Fields in Heterogeneous Confined Aquifers of Variable Thickness

Ching-Min Chang
National Central University College of Earth Sciences
Chuen-Fa Ni (nichuenfa@geo.ncu.edu.tw)
National Central University College of Earth Sciences https://orcid.org/0000-0002-2742-3308
We-Ci Li
National Central University College of Earth Sciences
Chi-Ping Lin
National Central University College of Earth Sciences
I-Hsian Lee
National Central University College of Earth Sciences

Research Article

Keywords: Nonstationary random fields, Fourier-Stieltjes representation, Variance of the depth-averaged hydraulic head, Variance of the integrated specific discharge

Posted Date: September 20th, 2021

DOI: https://doi.org/10.21203/rs.3.rs-919028/v1

Stochastic analysis of the variability of groundwater flow fields in heterogeneous confined aquifers of variable thickness

Ching-Min Chang[1] • Chuen-Fa Ni[1,*] • We-Ci Li[1] • Chi-Ping Lin[2] • I-Hsian Lee[2]

[1]Graduate Institute of Applied Geology, National Central University, Taoyuan, Taiwan

[2]Center for Environmental Studies, National Central University, Taoyuan, Taiwan

Submit to ***Stochastic Environmental Research and Risk Assessment*** for publication

[*]Corresponding author, *E-mail address*: nichuenfa@geo.ncu.edu.tw (C-F Ni)

Abstract

The problem of flow through heterogeneous confined aquifers of variable thickness is analyzed from a stochastic point of view. The analysis is carried out on the basis of the integrated equations of the depth-averaged hydraulic head and integrated specific discharge, which are developed by integrating the continuity equation and equation for the specific discharge over the thickness, respectively. A spectrally based perturbation approach is used to arrive at the general results for the statistics of the flow fields in the Fourier domain, such as the variance of the depth-averaged head, and the mean and variance of integrated discharge. However, the closed-form expressions are obtained under the condition of steady unidirectional mean flow in the horizontal plane. In developing stochastic solutions, the input hydraulic conductivity parameter is viewed as a spatial random field characterized by the theoretical spatial covariance function. The evaluation of the closed-form solutions focuses on the influence of the controlling parameters, namely as a geometrical parameter defining the variation of the aquifer thickness and the correlation scale of log hydraulic conductivity, on the variability of the fluid fields. The application of the present stochastic theory to predict the total specific discharge under uncertainty using the field data is also provided.

Keywords Nonstationary random fields • Fourier-Stieltjes representation • Variance of the depth-averaged hydraulic head • Variance of the integrated specific discharge

1 Introduction

There is an increasing demand for science-based approaches to the management and use of groundwater resources at regional scale (e. g., Zhou and Li 2011; Barthel and Banzhaf 2015; Sishodia et al. 2017; Pétré et al. 2019). Hydrologists are therefore often interested in the solutions of regional groundwater flow models. The solutions may be required for purpose of prediction and design. As such, it is important in constructing a regional flow model that may accurately represent the effects of hydrological changes on the behavior of the aquifer.

Groundwater flow at regional scale is concerned with the movement of flow through an aquifer whose lateral extent of the formation is much larger than the formation thickness (e. g., Nastev et al. 2008; Vassena et al. 2012; Rotiroti et al. 2019). When dealing with regional groundwater flow problems, it is more practical to treat the flow essentially horizontal and neglect the vertical component of the flow. That is, the flow behavior at regional scale can be appropriately described by a two-dimensional continuity equation, whereby the parameters such as the specific storage coefficient and hydraulic conductivity are replaced by the storativity and transmissivity, respectively. The output of the two-dimensional equation is then interpreted as the depth-averaged hydraulic head. The assumption of an essentially horizontal flow helps by reducing the effective dimension of the problem by one, which simplifies the problem, and the two-dimensional problem needs less detailed knowledge about the medium properties. Note that the analysis of regional groundwater flow based on the two-dimensional horizontal flow approximation is referred to as the hydraulic approach to flow in aquifers (Bear 1979; Bear and Cheng 2010).

Most research on essentially horizontal flow problems in confined aquifers considers the thickness of the aquifer to be uniform throughout the entire flow domain. However, natural aquifers often exhibit nonuniformity in the thickness of confined aquifers at a regional scale (Refsgaard 1997; Leray et al. 2012; Rotzoll et al. 2013; Andreasen et al. 2013). Hence, there arise pertinent questions as follows: (1) How can the existing model, which is limited to the flow through the confined aquifer of constant thickness, be generalized to the case of flow through the aquifer of variable thickness? (2) How does the thickness of the aquifer affect the flow field? These questions define the theme of this paper. The influence of the nonuniform thickness of confined aquifers on the flow behavior will be analyzed within a stochastic framework.

It is generally recognized that the movement of groundwater is strongly influenced by the complex heterogeneity of natural aquifer materials, the details of which cannot be precisely predicted. Therefore, for accurate predictions of the groundwater movement, a large number of measurements are required to represent the actual heterogeneity of the aquifer. This situation is, however, far from that encountered in practice. The amount of information on all coefficients and parameters appearing in the groundwater prediction model for accurate predictions is never sufficient, so that a certain degree of uncertainty (variability) about the average predictions must be accepted.

For the problems of flow in heterogeneous aquifers, a logical approach such as a stochastic methodology may be to ignore the details of the fine-scale variations and to develop a theoretical basis for the description of the large-scale flow behavior in terms of effective parameters (e.g., Gelhar 1986; Dagan and Neuman 1997; Christakos 2003). The next step is to quantify the degree of variability (uncertainty) about the predicted mean.

83 This approach will be appropriate if the overall scale of the problem is large compared to
84 the scale of the heterogeneity. The detailed theoretical development of the modeling of
85 the mean flow behavior and the variation about the predicted mean involved in the study
86 of subsurface-flow in heterogeneous aquifers may be referred to the textbooks such as
87 Dagan (1989), Gelhar (1993), Zhang (2002) and Rubin (2003). A stochastic methodology
88 will be used to arrive at the results of this work.

89 This paper begins with the development of integrated equation of the depth-averaged
90 hydraulic head, for an essentially horizontal flow in confined aquifers of variable
91 thickness. These provides a basis for a stochastic description of the statistics of the flow
92 fields. General results such as the variance of the depth-averaged head, and the mean and
93 variance of integrated discharge are obtained for the temporally and spatially varied flow
94 fields, but closed-form expressions are limited to the case of steady unidirectional mean
95 flow in the horizontal plane. The stochastic methodology employed to derive the
96 closed-form expressions is based on the representation theorem and Fourier-Stieltjes
97 representation. Focus of analysis is placed on the influence of the controlling parameters
98 on the variability of fluid field. The application of the present stochastic theory is
99 demonstrated by predicting the total specific discharge under uncertainty from the field
100 data. To our knowledge, the influence of aquifer thickness on the variability of flow field
101 has not been investigated in the literature so far because of the difficulty of using the
102 traditional approach. The stochastic approach presented in this study provides an efficient
103 way to analyze flow fields in confined aquifers with non-uniform thickness. It is our hope
104 that the present study will stimulate further research in this area.
105

2 Material and methods

2.1 Mathematical framework

The present research is concerned with a confined aquifer of variable thickness bounded by two confining beds. The governing equation of transient flow in confined aquifers in the absence of recharge can be written in the form (e.g., Bear 1979; de Marsily 1986) as

$$S_s \frac{\partial h}{\partial t} = \nabla \cdot [\boldsymbol{K} \nabla h] \tag{1}$$

where S_s is the specific storage coefficient of the aquifer, $\boldsymbol{K}$ is the hydraulic conductivity (tensor), $h=h(\boldsymbol{x},t)$ is the hydraulic head, and $\boldsymbol{x}$ (= (x_1,x_2,x_3)) is the spatial coordinate vector. Equation (1) is obtained from coupling the mass conservation equation with Darcy's law. For an isotropic, but inhomogeneous medium, Eq. (1) becomes

$$S_s \frac{\partial}{\partial t} h(x_1, x_2, x_3, t) = \frac{\partial}{\partial x_i} [K(x_1, x_2, x_3) \frac{\partial}{\partial x_i} h(x_1, x_2, x_3, t)] \qquad i = 1, 2, 3 \tag{2}$$

For later applications, it is convenient to choose one of the principal coordinates, x_3, perpendicular to the confining beds and the other two principal coordinates, x_1 and x_2, parallel to the plane of the confining beds. Integration of Eq. (2) along the x_3-axis and use of Leibniz' rule leads to the following general structure:

$$S_s \frac{\partial}{\partial t} \int_{b_1(x,y)}^{b_2(x,y)} h(x_1, x_2, x_3, t)\, dx_3 = \frac{\partial}{\partial x_i} \Big[\frac{\partial}{\partial x_i} \int_{b_1(x_1,x_2)}^{b_2(x_1,x_2)} K(x_1, x_2, x_3) h(x_1, x_2, x_3, t)\, dx_3 - \int_{b_1(x_1,x_2)}^{b_2(x_1,x_2)} h(x_1, x_2, x_3, t) \frac{\partial}{\partial x_i} K(x_1, x_2, x_3)\, dx_3 \Big]$$

$$- h(x_1, x_2, b_2, t) \frac{\partial}{\partial x_i} [K(x_1, x_2, b_2) \frac{\partial}{\partial x_i} b_2(x_1, x_2)] + h(x_1, x_2, b_1, t) \frac{\partial}{\partial x_i} [K(x_1, x_2, b_1) \frac{\partial}{\partial x_i} b_1(x_1, x_2)]$$

$$- q_v(x_1, x_2, b_2, t) + q_v(x_1, x_2, b_1, t) \qquad i = 1, 2 \tag{3a}$$

where $b_1(x_1,x_2)$ and $b_2(x_1,x_2)$ describe the surfaces of the fixed bottom and ceiling from the horizontal plane of reference, and

$$q_v(x_1, x_2, b_2, t) = -K(x_1, x_2, b_2) \frac{\partial}{\partial x_3} h(x_1, x_2, b_2, t) \tag{3b}$$

$$q_v(x_1, x_2, b_1, t) = -K(x_1, x_2, b_1) \frac{\partial}{\partial x_3} h(x_1, x_2, b_1, t) \tag{3c}$$

The last two terms in Eq. (3a) represent the leakage fluxes exchanged between the confined aquifer and its confining beds in the direction of x_3-axis. In the development of Eq. (3a), all the terms involved in the fluxes at the boundaries are removed from Eq. (3a) on the basis of the no-slip condition at the boundary. Equation (3a) is a depth-integrated continuity equation for an essentially horizontal flow in a confined aquifer of variable thickness.

By introducing the depth-averaged hydraulic head operator,

$$\tilde{h}(x_1, x_2, t) = \frac{1}{b_2(x_1, x_2) - b_1(x_1, x_2)} \int_{b_1(x_1, x_2)}^{b_2(x_1, x_2)} h(x_1, x_2, x_3, t)\, dx_3 \tag{4a}$$

and the assumption of $K = K(x_1,x_2)$, Eq. (3a) may be written as

$$\begin{aligned} S(x_1, x_2) \frac{\partial}{\partial t} \tilde{h}(x_1, x_2, t) = {} & \frac{\partial}{\partial x_i} \left[T(x_1, x_2) \frac{\partial}{\partial x_i} \tilde{h}(x_1, x_2, t) \right] + T(x_1, x_2) \frac{\partial}{\partial x_i} \ln B(x_1, x_2) \frac{\partial}{\partial x_i} \tilde{h}(x_1, x_2, t) \\ & + [\tilde{h}(x_1, x_2, t) - h(x_1, x_2, b_2, t)] \frac{\partial}{\partial x_i} [K(x_1, x_2, b_2) \frac{\partial}{\partial x_i} b_2(x_1, x_2)] \\ & - [\tilde{h}(x_1, x_2, t) - h(x_1, x_2, b_1, t)] \frac{\partial}{\partial x_i} [K(x_1, x_2, b_1) \frac{\partial}{\partial x_i} b_1(x_1, x_2)] \\ & - q_{x_3}(x_1, x_2, b_2, t) + q_{x_3}(x_1, x_2, b_1, t) \qquad i = 1, 2 \end{aligned} \tag{4b}$$

where $S(x_1,x_2)$ is the storage coefficient (or storativity) of the aquifer (= $S_sB(x_1,x_2)$), $B(x_1,x_2)$ = $b_2(x_1,x_2)$- $b_1(x_1,x_2)$ (an aquifer's thickness) and $T(x_1,x_2)$ is the transmissivity of the aquifer (=$K(x_1,x_2)B(x_1,x_2)$), interpreted as the depth-integrated hydraulic conductivity. Furthermore, introducing the assumption of vertical equipotentials (i.e., $h(x_1,x_2,b_2,t) \approx \tilde{h}(x_1,x_2,t) \approx h(x_1,x_2,b_1,t)$; Bear 1979; Bear and Cheng 2010) into Eq.(4b) yields

$$S(x_1,x_2)\frac{\partial}{\partial t}\tilde{h}(x_1,x_2,t) = \frac{\partial}{\partial x_i}\left[T(x_1,x_2)\frac{\partial}{\partial x_i}\tilde{h}(x_1,x_2,t)\right] + T(x_1,x_2)\frac{\partial}{\partial x_i}\ln B(x_1,x_2)\frac{\partial}{\partial x_i}\tilde{h}(x_1,x_2,t)$$

$$- q_{x_3}(x_1,x_2,b_2,t) + q_{x_3}(x_1,x_2,b_1,t) \qquad i = 1, 2 \tag{5}$$

Equation (5) indicates that the essentially horizontal flow is suitably described in terms of the average hydraulic head, taken over the thickness of the aquifer. The two aquifer properties characterizing the medium are the depth-integrated hydraulic conductivity and specific storage coefficient, namely transmissivity and storativity, respectively. Alternatively, in the absence of the leakage fluxes Eq. (5) may be rewritten as

$$\frac{S_s}{K(x_1,x_2)}\frac{\partial}{\partial t}\tilde{h}(x_1,x_2,t) = \frac{\partial^2}{\partial x_i^2}\tilde{h}(x_1,x_2,t) + \left[\frac{\partial}{\partial x_i}\ln K(x_1,x_2) + 2\frac{\partial}{\partial x_i}\ln B(x_1,x_2)\right]\frac{\partial}{\partial x_i}\tilde{h}(x_1,x_2,t) \qquad i = 1, 2$$

(6)

which is convenient for the stochastic analysis of the effect of the aquifer's thickness.

It is worth mentioning that the assumption of vertical equipotentials or, equivalently, the assumption of essential two-dimensional flow parallel to the confining beds, is valid when the variation of the aquifer's thickness is much smaller than the average thickness (Bear 1979; Bear and Cheng 2010). The error introduced by this assumption is very small in most cases of practical interest, which greatly simplifies the analysis of flow in confined aquifers.

Equation (6) serves as the starting point for the present study, where the spatial

variation of hydraulic conductivities in the continuum sense is treated as a random field characterized by the theoretical spatial covariance function. The random heterogeneity in hydraulic conductivity as an input parameter in Eq. (6) leads to the random heterogeneity in depth-averaged hydraulic head, the output of Eq. (6). Consequently, Eq. (6) is a stochastic differential equation with a stochastic output $\tilde{h}(x_1, x_2, t)$. In order to obtain a complete description of model output, one would have to specify its joint probability density function over the entire flow field. A more realistic approach, however, is to represent the resulting predictions in terms of certain statistical moments of the random output field and this is the task to be performed here. The mean or expected value (the first-moment) represents the optimum unbiased predictor of the output. The variance-covariance (the second-moment) of the output field serves to quantify predictive uncertainty (variability).

2.2 General derivation of variances of the head and integrated discharge

Representing each of random variables in Eq. (6), namely $\ln K$ and $\tilde{h}$, in terms of a mean and a zero-mean perturbation about the mean,

$$\ln K(x_1, x_2) = F + f(x_1, x_2) \tag{7}$$

$$\tilde{h}(x_1, x_2, t) = H(x_1, t) + h'(x_1, x_2, t) \tag{8}$$

results in the first-order stochastic partial differential equations for the mean depth-averaged head and the depth-averaged head perturbation, respectively, as

187 $$\frac{S_s}{e^F}\frac{\partial}{\partial t}H(x_1,t)=\frac{\partial^2}{\partial x_1^2}H(x_1,t)+2\frac{\partial}{\partial x_1}\ln B(x_1,x_2)\frac{\partial}{\partial x_1}H(x_1,t) \quad (9)$$

188 $$\frac{S_s}{e^F}\left[\frac{\partial}{\partial t}h'(x_1,x_2,t)-f\frac{\partial}{\partial t}H(x_1,t)\right]=\frac{\partial^2}{\partial x_i^2}h'(x_1,x_2,t)+2\frac{\partial}{\partial x_i}\ln B(x_1,x_2)\frac{\partial}{\partial x_i}h'(x_1,x_2,t)$$

189 $$+\frac{\partial}{\partial x_1}f(x_1,x_2)\frac{\partial}{\partial x_1}H(x_1,t) \qquad i=1,2 \quad (10)$$

190 In the derivation of Eqs. (9) and (10), F (the mean ln$K$) is treated as constant. Note that
191 since small changes in ln$K$ may correspond to large variations in K, there is an obvious
192 advantage to work in terms of ln$K$ rather than K. Unlike the classic stochastic equations
193 for the confined aquifer flow, the variable thickness of confined aquifer introduces the
194 second terms on the right-hand sides of Eqs. (9) and (10), respectively.

195 Equations (9) and (10) form a system of coupled partial differential equations in the
196 sense that one must know the behavior of the gradient of the mean depth-averaged
197 hydraulic head in order to solve Eq. (10). Upon the solution of Eq. (9), Eq. (10) may be
198 solved using Fourier-Stieltjes representations for the perturbed quantities in Eq. (10).
199 From the functional spectral relationship between the fluctuations in ln$K$ and $\tilde{h}$ (the
200 solution of Eq. (10)), it is then possible to determine the variance of the depth-averaged
201 hydraulic head within the following framework for known autocorrelation function of the
202 log-hydraulic conductivity:

203 $$\sigma_h^2(x_1,x_2,t)=E[h'(x_1,x_2,t)h'(x_1,x_2,t)] \quad (11)$$

204 Many applications require information such as the fluxes as a prelude to more
205 complex calculations. In addition, since solute transport is controlled by the underlying
206 velocity field, the statistical moments of the velocity field are essential for studying solute
207 transport process at the field scale. Therefore, the characteristics of specific discharge

variability are important in the analysis of groundwater related problems.

Similarly, applying Leibnitz' rule to the equation for the specific discharge through the confined aquifer of variable thickness under the aforementioned assumption of vertical equipotentials yields the vertically integrated specific discharge (total specific discharge) in the x_i direction as

$$Q_{x_i}(x_1,x_2,t) = -K(x_1,x_2)B(x_1,x_2)\frac{\partial}{\partial x_i}\tilde{h}(x_1,x_2,t) = -T(x_1,x_2)\frac{\partial}{\partial x_i}\tilde{h}(x_1,x_2,t) \tag{12}$$

The reader is referred to Bear and Cheng (2010) for a detailed derivation of Eq. (12). Due to the random hydraulic conductivity as an input parameter, Eq. (12) is the stochastic differential equation governing the random vertically integrated specific discharge through the confined aquifer of variable thickness.

Following the approach of Gelhar (1993), the mean flow characteristics of a heterogeneous confined aquifer can be evaluated by substituting Eqs. (7) and (8) into Eq. (12), taking the expected value of it, treating F as a constant, and disregarding the third-order perturbation terms

$$\overline{Q_{x_i}}(x_1,x_2,t) = E[Q_{x_i}(x_1,x_2,t)]$$

$$= -B(x_1,x_2)e^F E\left\{(1+f+\frac{1}{2}f^2+\Lambda)\frac{\partial}{\partial x_i}[H(x_1,x_2,t)+h'(x_1,x_2,t)]\right\}$$

$$\approx \overline{T}(x_1,x_2)\left\{J_i(x_1,x_2,t)(1+\frac{1}{2}\sigma_f^2) - E[f(x_1,x_2)\frac{\partial}{\partial x_i}h'(x_1,x_2,t)]\right\} \tag{13}$$

where $\overline{Q_{x_i}}$ is the mean integrated discharge, σ_f^2 is the variance of log-conductivity, $J_i = -\partial H/\partial x_i$, and

$$\overline{T}(x_1,x_2) = E[T(x_1,x_2)] = B(x_1,x_2)e^F \tag{14}$$

The variations of the integrated discharge about the mean can be found simply by

subtracting the mean expression of Eq. (13) from Eq. (12)

$$Q'_{x_i}(x_1,x_2,t) = Q_{x_i}(x_1,x_2,t) - E[Q_{x_i}(x_1,x_2,t)]$$

$$= -\bar{T}(x_1,x_2)[\frac{\partial}{\partial x_i}h'(x_1,x_2,t) - f(x_1,x_2)\,J_i(x_1,x_2,t)] \quad (15)$$

where terms involving the products of perturbed quantities have been neglected in the final expression. The variance of the integrated discharge may be determined by employing the representation theorem for the discharge perturbation as follows

$$\sigma^2_{Q_i}(x_1,x_2,t) = E[Q'_{x_i}(x_1,x_2,t)\,Q'_{x_i}(x_1,x_2,t)]$$

$$= \bar{T}^2(x_1,x_2)\Big\{E[\frac{\partial}{\partial x_i}h'(x_1,x_2,t)\frac{\partial}{\partial x_i}h'(x_1,x_2,t)] + J_i(x_1,x_2,t)\big(J_i(x_1,x_2,t)\,\sigma_f^2 - 2E[f(x_1,x_2)\frac{\partial}{\partial x_i}h'(x_1,x_2,t)]\big)\Big\}$$

(16)

Natural aquifer materials are heterogeneous in terms of their flow properties such as the hydraulic conductivity so that the local water flow rate can vary in different regions of the aquifer. The effect of heterogeneity can be accounted for by formulating the specific discharge problem in a stochastic framework. The mean specific discharge in Eq. (13) gives us an unbiased estimate of a system state in a heterogeneous medium, and the corresponding variance in Eq. (16) characterizes the uncertainty associated with the estimation. These two moments construct confidence intervals for the discharge field.

The following section is devoted to derive closed-form analytic expressions for the variance of the depth-averaged hydraulic head, the mean and variance of integrated specific discharge in Eqs. (11), (13) and (16), respectively, based on the Fourier-Stieltjes representation approach.

3 Results and discussion

To gain a clear insight into the impact of the aquifer's thickness, the following theoretical development restricts attention to the case of steady unidirectional mean flow (e. g., Naff and Vecchia 1986; Gelhar 1993; Rubin and Bellin 1994; Ni and Li 2006) in the x_1 direction through a confined aquifer whose thickness varies as $B(x_1) = b_0\exp(-\alpha x_1)$ (Hantush 1962b; Marino and Luthin 1982) where b_0 and α are positive geometrical parameters. Note that three types of expressions have been used in the literature to describe the thickness of the aquifer, such as linear (Hantush 1962a; Zamrsky et al., 2018), quadratic (Cuello et al. 2017; Zamrsky et al. 2018), and exponential (Hantush, 1962b; Marino and Luthin 1982) varying thickness expressions. As such, the two-dimensional aspect of the flow is entirely due to local deviations of the gradient from its mean. In practice, the flow is generally unsteady, but after a prolonged period of time, the head changes very slowly in time, and a steady state is practically reached.

Under the above assumptions, Eqs. (9) and (10) can be simplified, respectively, as

$$\frac{d^2}{dx_1^2}H(x_1) - 2\alpha\frac{d}{dx_1}H(x_1) = 0 \tag{17}$$

$$\frac{\partial^2}{\partial x_1^2}h'(x_1,x_2) + \frac{\partial^2}{\partial x_2^2}h'(x_1,x_2) - 2\alpha\frac{\partial}{\partial x_1}h'(x_1,x_2) = -\frac{\partial}{\partial x_1}f(x_1,x_2)\frac{d}{dx_1}H(x_1) \tag{18}$$

Equation (17) admits a representation of the mean depth-averaged head gradient of the form

$$J(x_1) = -\frac{d}{dx_1}H(x_1) = J_0\exp(2\alpha x_1) \tag{19}$$

where J_0 is a known value of $J(x_1)$ at the reference location $x_1 = 0$.

Furthermore, this work treats ln$K$ as a weakly stationary (second-order stationary)

random process and considers the autocovariance of fluctuations in ln$K$ field to be (Whittle 1954; Rodriguez-Iturbe and Mejia 1974; Gelhar 1977)

$$C_f(\xi) = \sigma_f^2 \beta\xi K_1(\beta\xi) \tag{20}$$

where ξ is the magnitude of the separation, $\beta = \pi/(2\lambda)$, λ is the correlation scale of ln$K$ field, and $K_1(\text{-})$ is the first-order modified Bessel function of second kind. Whittle (1954) stated that the covariance function in Eq. (20) is more suitable than the exponential form for the analysis of two-dimensional random processes. The spectrum associated with Eq. (20) is

$$S_{ff}(R_1, R_2) = \frac{\sigma_f^2 \beta^2}{\pi(R_1^2 + R_2^2 + \beta^2)^2} \tag{21}$$

where the R_i are the components of the wave number vector $\boldsymbol{R}$ (= (R_1, R_2)).

For every second-order stationary process f, there is a complex-valued, random distribution $Z_f(\boldsymbol{R})$ in the wave-number domain such that (e.g., Lumley and Panofsky 1964; Christakos 1992)

$$f(x_1, x_2) = \int_{-\infty}^{\infty}\int_{-\infty}^{\infty} \exp[i(R_1 x_1 + R_2 x_2)]\, dZ_f(R_1, R_2) \tag{22}$$

where $dZ_f(\boldsymbol{R})$ represents an orthogonal increment. Note that when the process f is non-stationary, the presentation (22) is no longer valid. On the other hand, with no restriction on stationarity in a random process, the process h' may be represented in the form (e.g., Priestley 1965; Ni et al. 2010; Ni et al. 2011)

$$h'(x_1, x_2) = \int_{-\infty}^{\infty}\int_{-\infty}^{\infty} \Lambda(x_1, x_2; R_1, R_2)\, dZ_f(R_1, R_2) \tag{23}$$

where $\Lambda(\text{-})$ is an oscillatory function in the sense of Priestley's definition (Priestley, 1965). In fact, Eq. (22) is simply a special case of Eq. (23) with the oscillatory function chosen as $\Lambda(x_1,x_2;R_1,R_2) = \exp(x_1R_1+x_2R_2)$. The use of the representation (23) for the process h' is due to the effect of variable thickness of the confined aquifer, causing the nonstationarity in the depth-averaged hydraulic head field. Note that nonuniformity in the mean head gradient caused by the effects of the physical flow boundaries (e.g., Oliver and Christakos 1995), uniformly distributed recharge (e.g., Rubin and Bellin 1994) and trends in mean log hydraulic conductivity fields (e.g., Ni and Li 2005) can also lead to nonstationarity in the statistics of flow fields in heterogeneous aquifer.

Substituting Eqs. (19), (22) and (23) into Eq. (18), it follows that

$$\frac{\partial^2}{\partial x_1^2}\Lambda(x_1,x_2;R_1,R_2)+\frac{\partial^2}{\partial x_2^2}\Lambda(x_1,x_2;R_1,R_2)-2\alpha\frac{\partial}{\partial x_1}\Lambda(x_1,x_2;R_1,R_2)=iR_1J_0\exp[2\alpha x_1+i(R_1x_1+R_2x_2)] \tag{24}$$

which admits the solution given by

$$\Lambda(x_1,x_2;R_1,R_2)=-iJ_0\frac{R_1}{R_1^2+R_2^2-i2\alpha R_1}\exp[2\alpha x_1+i(R_1x_1+R_2x_2)] \tag{25}$$

The solution applies only to a region of interest sufficiently far from the boundary so that its effect on head fluctuations is not felt. Combining Eq. (25) with Eq. (23) gives

$$h'(x_1,x_2)=-J_0e^{2\alpha x_1}\int_{-\infty}^{\infty}\int_{-\infty}^{\infty}\frac{iR_1}{R_1^2+R_2^2-i2\alpha R_1}\exp[i(R_1x_1+R_2x_2)]dZ_f(R_1,R_2) \tag{26}$$

3.1 Variance of depth-averaged hydraulic head

311 Application of the spectral representation theorem (Eq. (11)) for h' in Eq. (26) yields

312 $$\sigma_h^2(x_1) = J_0^2 e^{4\alpha x_1} \int_{-\infty}^{\infty}\int_{-\infty}^{\infty} \frac{R_1^2}{(R_1^2+R_2^2)^2 + 4\alpha^2 R_1^2} S_{ff}(R_1, R_2)\, dR_1\, dR_2 \tag{27}$$

313 Finally, the integral in Eq. (27) with respect to $\boldsymbol{R}$ is evaluated along with Eq. (21) to yield
314 the closed-form expression for the variance of depth-averaged hydraulic head as

315 $$\sigma_h^2(x_1) = \frac{1}{4}\sigma_f^2 \frac{J_0^2}{\alpha^2} e^{4\alpha x_1}\left\{1 - \frac{\eta}{(\eta^2-1)^{3/2}}\left[\eta\sqrt{\eta^2-1} - \ln(\eta + \sqrt{\eta^2-1})\right]\right\} \tag{28}$$

316 where $\eta = \pi/(4\alpha\lambda)$. It is apparent from Eqs. (19) and (28) that the statistics of random
317 depth-averaged head fields is nonstationary. That is, the nonuniform thickness of the
318 confined aquifer introduces nonuniformity in the mean depth-averaged head gradient and,
319 in term, nonstationarity in the statistics of the head fields.

320 Figure 1 displays dimensionless results of the variance of depth-averaged hydraulic
321 head in Eq. (28) versus the α-parameter for various values of the positions. It can be
322 clearly seen that the larger the α parameter, the greater the variability of depth-averaged
323 hydraulic head. Notice from Eq. (18) that the variation of fluctuations in ln$K$ appears as a
324 forcing term that derives the variation of fluctuations in depth-averaged head. The
325 behavior of an increase in the variability of head with the α-parameter may therefore be
326 explained by the analysis of the input-output spectrum relation. From Eqs. (11) and (23),
327 an evolutionary power spectral density of a non-stationary process, S_{hh}(-), can be defined
328 as, according to (Priestley 1965)

329 $$\sigma_h^2(x_1) = \int_{-\infty}^{\infty}\int_{-\infty}^{\infty} S_{hh}(x_1; R_1, R_2)\, dR_1\, dR_2 = \int_{-\infty}^{\infty}\int_{-\infty}^{\infty} \left|A(x_1, x_2; R_1, R_2)\right|^2 S_{ff}(R_1, R_2)\, dR_1\, dR_2 \tag{29}$$

330 which reveals from Eq. (25) that

$$S_{hh}(x_1;R_1,R_2)=\left|\Lambda(x_1,x_2;R_1,R_2)\right|^2 S_{ff}(R_1,R_2)=\frac{J_0^2 e^{4\alpha x_1}R_1^2}{(R_1^2+R_2^2)^2+4\alpha^2 R_1^2}S_{ff}(R_1,R_2) \tag{30}$$

Since the head variance may be interpreted as a measure of the total energy of the nonstationary process at the position x_1, Eq. (29) gives a decomposition of total energy in which the contribution from wave numbers R_1, R_2 is $S_{hh}(x_1;R_1,R_2)\mathrm{d}R_1\mathrm{d}R_2$. The result in Fig. 2, a plot of the dimensionless oscillatory function in Eq. (30) versus the dimensionless wave number, shows that the contribution of the local spectrum of ln$K$ processes to that of the head processes is enhanced by a larger α-parameter, which, in turn, leads to a higher depth-averaged head variability. It is worth noting that $\left|\Lambda(x_1,x_2;R_1,R_2)\right|^2$ acts as a low-pass filter in the wave number domain which attenuates the high wave number portion of the spectrum. The filtering associated with the flow process smooths-out much of the small-scale variations caused by the input ln$K$ parameter. Physically, this feature implies that the head field is much smoother than the ln$K$ field. The spatial correlation of the head perturbations is larger than that of the conductivity perturbations.

In addition, using Eq. (22) along with the fluctuations in depth-averaged head given by Eq. (26), the cross-correlation between the ln$K$ perturbation and the perturbation in depth-averaged head can be obtained as

$$E[fh']=\frac{1}{2}\sigma_f^2\frac{J_0}{\alpha}e^{2\alpha x_1}\left\{1-\frac{\eta}{(\eta^2-1)^{3/2}}\left[\eta\sqrt{\eta^2-1}-\ln(\eta+\sqrt{\eta^2-1})\right]\right\} \tag{31}$$

The result of Eq. (31) is presented graphically in Fig. 3, which indicates an increase in the f-h' cross-correlation with the α-parameter. The f-h' cross-correlation may be interpreted as the projection of amplitude of log-conductivity fluctuations onto that of head fluctuations. Since the spatial variation of hydraulic conductivities is the source of the

352 depth-averaged head variation, a larger *f*-*h*′ cross-correlation increases the correlation of
353 head perturbations. This provides an alternative way to explain the behavior shown in Fig.
354 1.

355 Another aspect of interest is the impact of the correlation scale of ln*K* field on the
356 variability of depth-averaged hydraulic head. An evaluation of the effect of the
357 correlation scale of ln*K* field is shown in Fig. 4. As expected, a larger correlation scale
358 causes greater variability in the depth-averaged head. Stochastic processes with a larger
359 correlation scale tend to show an increase in values after previous increases, and a
360 decrease after previous decreases. The data profile with the larger correlation scale
361 exhibits quite clear trends with relatively little noise, i.e. a fewer number of mean value
362 crossings. As such, a larger ln*K* correlation scale means larger inclusions, which, in turn,
363 leads to larger deviations of the depth-averaged head from the mean head surface.
364

365 3.2 Mean and variance of integrated specific discharge

366

367 In the case of steady unidirectional mean flow, the mean and variance of integrated
368 specific discharge (total discharge) in Eqs. (13) and (16), respectively, take the form

369 $$\overline{Q}_{x1}(x_1) = B(x_1)e^{F}\left\{J_0 e^{2\alpha x_1}(1+\frac{1}{2}\sigma_f^2) - E[f(x_1,x_2)\frac{\partial}{\partial x_1}h'(x_1,x_2)]\right\} \quad (32)$$

370 $$\overline{Q}_{x2}(x_1) = -B(x_1)e^{F}E[f(x_1,x_2)\frac{\partial}{\partial x_2}h'(x_1,x_2)] \quad (33)$$

371 $$\sigma_{Q_1}^2(x_1,x_2) = B^2(x_1)e^{2F}\left\{E[\frac{\partial}{\partial x_1}h'(x_1,x_2)\frac{\partial}{\partial x_1}h'(x_1,x_2)] + J_0 e^{2\alpha x_1}\left(J_0 e^{2\alpha x_1}\sigma_f^2 - 2E[f(x_1,x_2)\frac{\partial}{\partial x_1}h'(x_1,x_2)]\right)\right\} \quad (34)$$

372 $$\sigma_{Q_2}^2(x_1,x_2) = B^2(x_1)e^{2F}E[\frac{\partial}{\partial x_2}h'(x_1,x_2)\frac{\partial}{\partial x_2}h'(x_1,x_2)] \quad (35)$$

373 The terms, $E[f(x_1,x_2)\frac{\partial}{\partial x_i}h'(x_1,x_2,t)]$ in Eqs. (32) and (33), and

374 $E[\frac{\partial}{\partial x_i}h'(x_1,x_2,t)\frac{\partial}{\partial x_i}h'(x_1,x_2,t)]$ in Eqs. (34) and (35), are expressed, respectively, by

375 making use of the representation theorem as follows

376 $$E[f(x_1,x_2)\frac{\partial}{\partial x_1}h'(x_1,x_2)] = -J_0 e^{2\alpha x_1}\int_{-\infty}^{\infty}\int_{-\infty}^{\infty}\frac{iR_1(iR_1+2\alpha)}{R_1^2+R_2^2-i2\alpha R_1}S_{ff}(R_1,R_2)\,dR_1\,dR_2 \tag{36}$$

377 $$E[f(x_1,x_2)\frac{\partial}{\partial x_2}h'(x_1,x_2)] = -J_0 e^{2\alpha x_1}\int_{-\infty}^{\infty}\int_{-\infty}^{\infty}\frac{R_1R_2}{R_1^2+R_2^2-i2\alpha R_1}S_{ff}(R_1,R_2)\,dR_1\,dR_2 \tag{37}$$

378 $$E[\frac{\partial}{\partial x_1}h'(x_1,x_2)\frac{\partial}{\partial x_1}h'(x_1,x_2)] = J_0^2 e^{4\alpha x_1}\int_{-\infty}^{\infty}\int_{-\infty}^{\infty}\frac{R_1^2(R_1^2+4\alpha^2)}{(R_1^2+R_2^2)^2+4\alpha^2R_1^2}S_{ff}(R_1,R_2)\,dR_1\,dR_2 \tag{38}$$

379 $$E[\frac{\partial}{\partial x_2}h'(x_1,x_2)\frac{\partial}{\partial x_2}h'(x_1,x_2)] = J_0^2 e^{4\alpha x_1}\int_{-\infty}^{\infty}\int_{-\infty}^{\infty}\frac{R_1^2R_2^2}{(R_1^2+R_2^2)^2+4\alpha^2R_1^2}S_{ff}(R_1,R_2)\,dR_1\,dR_2 \tag{39}$$

380 Equations (36)-(39) can be evaluated analytically for a given S_{ff} in Eq. (21). The

381 mean and variances are obtained from Eqs. (32)-(35), respectively, in the closed-form

382 after the computation of Eqs. (36)-(39)

383 $$\overline{Q_{x_1}}(x_1) = T_0 J_0 e^{\alpha x_1}\left\{1-\sigma_f^2\left[\frac{1}{2}+\frac{\eta}{\varepsilon^3}\left(-2\eta\varepsilon^3\ln(2\eta)+\ln(\phi_1)[1-\frac{3}{2}\eta^2+\eta^4]+\ln(\phi_2)\eta^2[\frac{3}{2}-\eta^2]\right)\right]\right\} \tag{40}$$

384 $$\overline{Q_{x_2}}(x_1) = 0 \tag{41}$$

385 $$\sigma_{Q_1}^2(x_1) = \sigma_f^2 T_0^2 J_0^2 e^{2\alpha x_1}\frac{\eta^2}{\varepsilon^3}\left\{\varepsilon^3\left[1+(3-4\eta^2)\ln(2\eta)\right]+\ln(\phi_1)\left[-\frac{1}{\eta}+3\eta-\frac{9}{2}\eta^3+2\eta^5\right]\right.$$

386 $$\left.+\ln(\phi_2)\eta\left[-3+\frac{9}{2}\eta^2-2\eta^4\right]\right\} \tag{42}$$

$$\sigma^2_{Q_2}(x_1) = \sigma_f^2 T_0^2 J_0^2 e^{2\alpha x_1} \frac{\eta^2}{\varepsilon}\left\{\varepsilon\left[-1+(4\eta^2-1)\ln(2\eta)\right]+\eta(2\eta^2-\frac{3}{2})[\ln(\phi_2)-\ln(\phi_1)]\right\} \quad (43)$$

where $T_0 = b_0 e^F$, $\varepsilon = (\eta^2\text{-}1)^{1/2}$, $\phi_1 = \eta+\varepsilon$, and $\phi_2 = \eta-\varepsilon$.

Figures 5 through 7 show the effect of the α-parameter on the mean integrated specific discharge and variability of integrated discharge in the directions of x_1 and x_2, respectively. These figures clearly indicate that introduction of a larger α-parameter leads to greater mean and variability of integrated specific discharge. As shown in previous sections, nonuniformity in the mean flow field introduced by the spatial variable thickness of the confined aquifer leads to nonstationarity in statistics of the head fields. Consequently, the statistics of the integrated specific discharge fields is nonstationary (position-dependent). Due to this dependence, an effective transmissivity throughout the flow domain does not exist following the rigorous definition of effective properties (e.g., Dagan 1989), representing the aquifer's material properties. That is, the heterogeneous material cannot be replaced by a homogeneous one of an effective property. When the integrated discharge divided by the mean head gradient varies spatially, it is sometimes referred to as the pseudo-effective parameter (e. g., Sanchez-Vila 1997), apparent transmissivity (e. g., Dagan 2001) or equivalent transmissivity (e. g., Rubin 2003).

By the representation theorem for the perturbation of integrated discharge Q'_{x_i}, the variance of integrated discharge in the *i*-direction can be written in the following simple form as

$$\sigma^2_{Q_i}(x_1) = \int_{-\infty}^{\infty}\int_{-\infty}^{\infty} S_{Q_i Q_i}(x_1; R_1, R_2)\, dR_1\, dR_2 \quad (44)$$

where $S_{Q_iQ_i}$(-) is the evolutionary power spectral density of the integrated discharge in the i-direction. Combining this with Eqs. (16), (22) and (23) yields

$$S_{Q_1Q_1}(x_1;R_1,R_2)=\left|\Lambda_{Q_1}(x_1;R_1,R_2)\right|^2 S_{ff}(R_1,R_2)=T_0^2J_0^2e^{2\alpha x_1}\frac{R^4-2R^2R_1^2+R_1^4}{R^4+4\alpha^2R_1^2}S_{ff}(R_1,R_2) \quad (45)$$

$$S_{Q_2Q_2}(x_1;R_1,R_2)=\left|\Lambda_{Q_2}(x_1;R_1,R_2)\right|^2 S_{ff}(R_1,R_2)=T_0^2J_0^2e^{2\alpha x_1}\frac{R_1^2R_2^2}{R^4+4\alpha^2R_1^2}S_{ff}(R_1,R_2) \quad (46)$$

where $R^2 = R_1^2 + R_2^2$. The incremental $S_{Q_iQ_i}(x_1;R_1,R_2)\mathrm{d}R_1\mathrm{d}R_2$ in Eq. (44) describes a wave number decomposition of the total energy of the process Q'_{x_i}. It can be demonstrated from the plots of Eqs. (45) and (46) in the wave number domain that the terms $\left|\Lambda_{Q_1}(x_1;R_1,R_2)\right|^2$ and $\left|\Lambda_{Q_2}(x_1;R_1,R_2)\right|^2$ in Eqs. (45) and (46), respectively, grow with the α-parameter. This means that the contribution to the spectrum of the integrated discharge from the space variation of the local spectrum of ln$K$ processes grow with the α-parameter, resulting in a higher variability of the integrated discharge for a larger α-parameter (see Figs. 6 and 7). In addition, similar to the filtering role of $\left|\Lambda(x_1,x_2;R_1,R_2)\right|^2$ in Eq. (30), $\left|\Lambda_{Q_1}(x_1;R_1,R_2)\right|^2$ and $\left|\Lambda_{Q_2}(x_1;R_1,R_2)\right|^2$ attenuate the high wave number portions of the spectrum in the x_1 and x_2 directions, respectively. The integrated discharge perturbations are correlated over a larger distance than the conductivity perturbations.

3.3 The case of increasing thickness of the confined aquifer

The analysis leading to the closed-form solutions is limited to the case of flow in a

confined aquifer whose thickness decreases in the x_1-direction. In the case of increasing thickness in the x_1-direction ($B(x_1) = b_0\exp(\alpha x_1)$, where b_0 and α are positive constants), the resultant expressions for the depth-averaged head, and mean and variance of integrated specific discharge are similar to those obtained when the aquifer's thickness decreases in the x_1-direction, with the exception that the term $\exp(\alpha x_1)$ is replaced by $\exp(-\alpha x_1)$ in Eqs. (28), (40), (42) and (43), namely

$$\sigma_h^2(x_1) = \frac{1}{4}\sigma_f^2 \frac{J_0^2}{\alpha^2} e^{-4\alpha x_1}\left\{1 - \frac{\eta}{(\eta^2-1)^{3/2}}\left[\eta\sqrt{\eta^2-1} + \ln(\eta+\sqrt{\eta^2-1})\right]\right\} \tag{47}$$

$$\overline{Q}_{x_1}(x_1) = T_0 J_0 e^{-\alpha x_1}\left\{1 - \sigma_f^2\left[\frac{1}{2} + \frac{\eta}{\varepsilon^3}\left(-2\eta\varepsilon^3\ln(2\eta) + \ln(\phi_1)[1 - \frac{3}{2}\eta^2 + \eta^4] + \ln(\phi_2)\eta^2[\frac{3}{2} - \eta^2]\right)\right]\right\} \tag{48}$$

$$\sigma_{Q_1}^2(x_1) = \sigma_f^2 T_0^2 J_0^2 e^{-2\alpha x_1}\frac{\eta^2}{\varepsilon^3}\left\{\varepsilon^3\left[1 + (3-4\eta^2)\ln(2\eta)\right] + \ln(\phi_1)\left[-\frac{1}{\eta} + 3\eta - \frac{9}{2}\eta^3 + 2\eta^5\right]\right.$$

$$\left. + \ln(\phi_2)\eta\left[-3 + \frac{9}{2}\eta^2 - 2\eta^4\right]\right\} \tag{49}$$

$$\sigma_{Q_2}^2(x_1) = \sigma_f^2 T_0^2 J_0^2 e^{-2\alpha x_1}\frac{\eta^2}{\varepsilon}\left\{\varepsilon\left[-1 + (4\eta^2-1)\ln(2\eta)\right] + \eta(2\eta^2 - \frac{3}{2})[\ln(\phi_2) - \ln(\phi_1)]\right\} \tag{50}$$

These equations suggest that the α-parameter plays a role in reducing the variance of the depth-averaged head, and mean and variance of the integrated specific discharge in the case of an increasing aquifer's thickness in the x_1-direction.

3.4 Differences between traditional and current approaches

It is important to recognize some significant differences between traditional and current approaches to describing flow in two-dimensional confined aquifers. The traditional

approach to regional groundwater flow problems assumes $h(x_1,x_2,x_3) \approx h(x_1,x_2)$ and introduces the depth-integrated hydraulic conductivity operator

$$T(x_1, x_2) = \int_{b_1(x_1, x_2)}^{b_2(x_1, x_2)} K(x_1, x_2, x_3)\, dx_3 \tag{51}$$

to map groundwater flow equation from three dimensions to two. This means that the effects of the variation of K in x_3-direction and the aquifer thickness are implicit in the term $T(x_1,x_2)$. As such, the diffusion equation can be approximated as

$$S(x_1, x_2)\frac{\partial}{\partial t}h(x_1, x_2, t) = \frac{\partial}{\partial x_i}[T(x_1, x_2,)\frac{\partial}{\partial x_i}h(x_1, x_2, t)] \qquad i = 1, 2 \tag{52}$$

Since Eq. (52), along with Eq. (51), is originally designed for the analysis of flow field in a confined aquifer with uniform thickness, it is very difficult to assess the influence of thickness on the flow field with them. An example that outlines the evaluation of the head variance using Eq. (52) is given below.

Spectral analysis of two-dimensional steady-state groundwater flow in a confined aquifer was performed by Mizell et al. (1982). Under the assumption of a unidirectional mean flow, the head variance is given by (Mizell et al. 1982)

$$\sigma_{\Phi}^2(x_1) = J_1^2 \int_{-\infty}^{\infty}\int_{-\infty}^{\infty} \frac{R_1^2}{(R_1^2 + R_2^2)^2} S_{yy}(R_1, R_2)\, dR_1 dR_2 \tag{53}$$

where $J_1 = -dE[h]/dx_1$, $S_{yy}(-)$ is the spectrum of fluctuations in y and $y = \ln T$. When the hydraulic conductivity field is a second-order stationary process, the covariance function for the transmissivity field defined by Eq. (51) is of the form (Vanmarke 1983)

$$C_T(\xi_1,\xi_2) = 2\int_0^B (B-\xi_3)\, C_K(\xi_1,\xi_2,\xi_3)\, d\xi_3 \tag{54}$$

where $\boldsymbol{\xi}$ (=(ξ_1, ξ_2, ξ_3)) is the separation vector, B is the depth of the aquifer and C_K(-) is the covariance function of K. Following the approach of Gutjahr et al. (1978), the relationship between the covariance function of ln$T$ and that of T can be determined as

$$C_y(\xi_1,\xi_2) = \ln\left[1 + 2\frac{C_T(\xi_1,\xi_2)}{e^{2Y}\Theta}\right] \tag{55a}$$

where $Y = E[\ln T]$,

$$\Theta = 1 + \sqrt{1 + 4\frac{\sigma_T^2}{(e^Y)^2}} \tag{55b}$$

and σ_T^2 is the variance of T. The spectrum S_{yy} of fluctuations in ln$T$ can be obtained by taking the inverse Fourier transform of C_y in Eq. (55a), i.e.,

$$S_{yy}(R_1,R_2) = \frac{1}{(2\pi)^2}\int_{-\infty}^{\infty}\int_{-\infty}^{\infty} \exp[-i(R_1\xi_1 + R_2\xi_2)]\, C_y(\xi_1,\xi_2)\, d\xi_1 d\xi_2 \tag{56}$$

Finally, the head variance considering the variable aquifer thickness can be determined by substituting Eqs. (54)-(55) into Eq. (56) for the Fourier transform inversion and after the inversion, substituting the result into Eq. (53) and then integrating over the wavenumber domain.

On the other hand, this work uses the hydraulic approach (Bear 1979; Bear and Cheng 2010), namely the assumption of $K(x_1,x_2,x_3) \approx K(x_1,x_2)$ and introduction of a depth-averaged head operator (Eq. (4a)), to reduce the three-dimensional diffusion equation to two-dimensional one:

$$S_s \frac{\partial}{\partial t}\tilde{h}(x_1,x_2,t) = \frac{1}{B(x_1,x_2)}\frac{\partial}{\partial x_i}\left[K(x_1,x_2)B(x_1,x_2)\frac{\partial}{\partial x_i}\tilde{h}(x_1,x_2,t)\right] + K(x_1,x_2)\frac{\partial}{\partial x_i}\ln B(x_1,x_2)\frac{\partial}{\partial x_i}\tilde{h}(x_1,x_2,t) \qquad i = 1, 2$$

(57)

which is the rewrite of Eq. (5) in the absence of the leakage fluxes. The effect of variation of K in x_3-direction is implicitly reflected in the depth-averaged head term $\tilde{h}(x_1, x_2, t)$. Equation (57) provides an efficient way for the analysis of flow fields in confined aquifers of non-uniform thickness.

In addition, the common observations of flow in porous media are hydraulic head measurements from wells screened over extended sections of the medium. The measurement at a given location represents approximately a depth-averaged actual hydraulic head, resulting from flow through a three-dimensional hydraulic conductivity field, over the thickness of the medium. This means that the depth-averaged head representation used in this work is consistent with what is observed from the fields. The problem solved in this work is practical.

3.5 Application in the prediction of total discharge considering uncertainty

Many practical applications of groundwater modeling involve predictions of total flow discharge over a relative large space scale, where only limited field data are available. There will be a great deal of uncertainty in the application of the solution of the mean model (or the deterministic model) as an estimate in field situations. An important feature of the stochastic approach described here is its essentially predictive character. The

504 variance Eq. (42) (or Eq. (49)) can be regarded as a quantitative measure of the
505 uncertainty associated with the prediction in field situations using the mean model. As
506 such, Eq. (40) (or Eq. (48)) ± twice the square root of Eq. (42) (or Eq. (49)) (standard
507 deviations) offers a useful basis for predicting the total discharge under uncertainty. Below
508 is an example to illustrate how this can be done using the field data.

509 To apply the present stochastic model to a particular area or region, such as the
510 Patuxent aquifer system in Anne Arundel county, Maryland, the specific parameters such
511 as the geometrical parameters describing the thickness of the confined aquifer (b_0 and α)
512 and the correlation scale of ln$K$ field (λ) must be estimated. For the analyses that
513 followed, the estimation of these parameters is based on the field data presented in
514 Andreasen et al. (2013) and Andreasen (2017).

515 Figure 8a and b show the variation in aquifer thickness and the distribution of
516 hydraulic conductivity as a function of distance from the aquifer outlet in the x_1 direction,
517 respectively. The data points in Fig. 8a are interpolated from Fig. 4 of Andreasen et al.
518 (2013). The curve with the best fit to the data points is given by

519 $$B(x_1) = 87 \times exp(0.000018 \times x_1) \tag{58}$$

520 The data points in Fig. 8b are obtained from the interpolated transmissivity from Fig. 8 of
521 Andreasen (2017) divided by the best-fit B (Eq. (58)).

522 If the number of samples for the hydraulic conductivity measurements is not large
523 enough, the variogram, an alternative description of the structure of the random hydraulic
524 conductivity field, can be used to estimate the variance and correlation scale of the ln$K$
525 field. For the case where the ln$K$ process is second-order stationary, the covariance
526 function and the variogram are linearly related by (Matheron 1971; de Marsily 1986)

$$\gamma_f(\xi) = \sigma_f^2 - C_f(\xi) \tag{59}$$

where $\gamma_f(\text{-})$ is the variogram of ln$K$ field. For the following analyses, the traditional experimental variogram estimator is used, defined as follows (de Marsily 1986; Kovitz and Christakos 2004):

$$\gamma_f(\xi) = \frac{1}{2N}\sum_{i=1}^{N}(\ln K_i - \ln K_j)^2 \tag{60}$$

where lnK_i and lnK_j are two measurements separated by a distance (separation) ξ and N is the number of pairs of data points in a selected separation interval. The points shown in Fig. 9 represent the experimental variogram of ln$K$ in the x_1-direction calculated from Eq. (60) and the hydraulic conductivity measurements described in Fig. 8b. From the fit of the theoretical variogram (i.e., the combination of Eq. (59) and Eq. (20)) to the experimental variogram Eq. (60), the variance and correlation scale of ln$K$ field are determined as σ_f^2 = 0.000173 and λ = 128 m, respectively. As shown in Fig. 9, the line that best fits the experimental variogram is used to estimate the variance and correlation scale of the log-conductivity field.

Finally, based on the specific parameters identified above, the predicted mean longitudinal total discharge (Eq. (48)) and associated standard deviation (square root of Eq. (49)) are presented in Fig. 10, where the mean and standard deviation of total discharge are normalized by $b_0 e^F J_0$. The general stochastic framework outlined here has potential applications in predictions over relatively large spatial scales where direct observations of such a dependent variable are not feasible.

4 Conclusions

549

550 Taking into account the influence of the thickness, the integrated equations of the
551 depth-averaged hydraulic head and integrated specific discharge are generated for flow
552 through confined aquifers of nonuniform thickness. They are based on the integration of
553 the continuity equation and equation for the specific discharge over the thickness,
554 respectively. The application of stochastic methodology for solving the integrated
555 equations leads to the general results for the statistics of the flow field in the Fourier
556 domain, such as the variance of the depth-averaged head, and the mean and variance of
557 integrated discharge. The closed-form expressions are obtained for the case of steady
558 unidirectional mean flow in the horizontal plane, which, however, allow to evaluate the
559 influence of the aquifer thickness on the variability of the flow field. The application of
560 the present stochastic theory in predicting the total specific discharge under uncertainty in
561 the field is also demonstrated.

562 The novel aspects of this work appear to be the theoretical development based on
563 Fourier-Stieltjes nonstationary representation and closed-form solutions for the statistics
564 of the flow field in confined aquifers of nonuniform thickness. There is certainly a need
565 to model these variables for applications to the groundwater resources management at
566 regional scale. In addition, the present study provides an efficient way to evaluate the
567 influence of thickness on flow fields using a hydraulic approach, while it is very difficult
568 to do so using a traditional approach.

569 The analysis of our closed-form solutions reveals that in the case of aquifers with
570 decreasing thickness the α-parameter has a positive impact on the variability of the flow
571 field. The α-parameter acts as a low-pass filter which smooths out much of the

572 small-scale variations caused by the input ln$K$ parameter. Therefore, the larger the
573 α-parameter, the greater the variability of the depth-averaged hydraulic head and
574 integrated specific discharge. A larger ln$K$ correlation scale means fewer mean crossings
575 for the depth-averaged head process around the mean head value, resulting in a larger
576 variability of the depth-averaged head field. In addition, an introduction of the
577 α-parameter leads to nonstationarity in the statistics of the head field and thus to a
578 position-dependent mean integrated specific discharge. On the other hand, in aquifers
579 with increasing thickness the α-parameter plays a role in reducing the variability of the
580 flow field.
581
582 **Acknowledgements** Research leading to this paper has been partially supported by
583 the grant from the Taiwan Ministry of Science and Technology under the grants MOST
584 108-2638-E-008 -001 -MY2, MOST 108-2625-M-008 -007, and MOST 107-2116-M-008
585 -003 -MY2.
586
587 **Conflict of interest** The authors have no conflicts of interest to declare that are
588 relevant to the content of this article.
589
590 ## References
591
592 Andreasen DC, Staley AW, Achmad G (2013) Maryland Coastal Plain aquifer
593 information system-Hydrogeologic framework: Maryland Geological Survey
594 Open-File Report 12-02-20.

595 Andreasen DC (2017) Effects of projected (2086) groundwater withdrawals on
596 management water levels and domestic wells in Anne Arundel County, Maryland.
597 Maryland Geological Survey Open-File Report 17-02-01.
598 Barthel R, Banzhaf S (2015) Groundwater and surface water interaction at the
599 regional-scale - A review with focus on regional integrated models. Water Resour
600 Manag 30(1):1-32.
601 Bear J (1979) Hydraulics of Groundwater. McGraw-Hill, New York.
602 Bear J, Cheng AH-D (2010) Modeling Groundwater Flow and Contaminant Transport,
603 Springer, Dordrecht.
604 Christakos G (1992) Random field models in earth sciences. Academic, San Diego.
605 Christakos G (2003). Another look at the conceptual fundamentals of porous media
606 upscaling. Stoch Environ Res Risk Assess 17(5):276-290.
607 Cuello JE, Guarracino L, Monachesi LB (2017) Groundwater response to tidal
608 fluctuations in wedge-shaped confined aquifers. Hydrogeol J 25(5):1509-1515.
609 Dagan G (1989) Flow and Transport in Porous Formations. Springer, New York, N. Y.
610 Dagan G, Neuman SP, ed. (1997) Subsurface Flow and Transport: A Stochastic
611 Approach. Cambridge University Press, UK.
612 Dagan G (2001) Effective, equivalent and apparent properties of heterogeneous media, in
613 Mechanics for a New Millennium. edited by Aref H and Phillips JW, 473-485,
614 Springer, New York.
615 de Marsily G (1986) Quantitative hydrogeology: Groundwater hydrology for engineers.
616 Academic Press, Orlando, FL.
617 Gelhar LW (1977) Effects of hydraulic conductivity variations on groundwater flows.

618 Proceedings Second International Symposium on Stochastic Hydraulics, Lund,
619 Sweden, in Hydraulic Problems Solved by Stochastic Methods, Water Resources
620 Publications, Fort Collins, 409-431.
621 Gelhar LW (1986) Stochastic subsurface hydrology from theory to applications. Water
622 Resour Res 22(9S):135S-145S.
623 Gelhar LW (1993) Stochastic Subsurface Hydrology. Prentice Hall, Englewood Cliffs,
624 New Jersey.
625 Gutjahr AL, Gelhar LW, Bakr AA, MacMillan JR (1978) Stochastic analysis of spatial
626 variability in subsurface flows: 2. Evaluation and application. Water Resour Res
627 14(5):953-959.
628 Hantush MS (1962a) Flow of ground water in sands of non-uniform thickness, part 2.
629 Approximate theory. J Geophys Res 67(4):711-720.
630 Hantush MS (1962b) Flow of ground water in sands of nonuniform thickness, part 3. Flow
631 to wells. J Geophys Res 67(4):1527-1534.
632 Kovitz JL, Christakos G (2004) Spatial statistics of clustered data. Stoch Environ Res
633 Risk Assess 18(3):147-166.
634 Leray S, de Dreuzy J-R, Bour O, Labasque T, Aquilina L (2012) Contribution of age data
635 to the characterization of complex aquifers. J Hydrol 464-465:54-68.
636 Lumley JL, Panofsky HA (1964) The structure of atmospheric turbulence. John Wiley,
637 New York.
638 Marino MA, Luthin JN (1982) Seepage and Groundwater. Elsevier, New York.
639 Mathero, G (1971) The theory of regionalized variables and its applications. Centre de
640 Morphol Math de Fontainebleau, Fontainebleau, France.

641 Mizell SA, Gutjahr AL, Gelhar LW (1982) Stochastic analysis of spatial variability in
642 two-dimensional steady groundwater flow assuming stationary and nonstationary
643 heads. Water Resour Res 18(4):1053-1067.
644 Naff RL, Vecchia AV (1986) Stochastic analysis of three-dimensional flow in a bounded
645 domain. Water Resour Res 22(5):695-704.
646 Nastev M, Morin R, Godin R, Rouleau A (2008) Developing conceptual hydrogeological
647 model for Potsdam sandstones in southwestern Quebec, Canada. Hydrogeol J
648 16(2):373-388.
649 Ni C-F, Li S-G (2005) Simple closed form formulas for predicting groundwater flow
650 model uncertainty in complex, heterogeneous trending media. Water Resour Res
651 41(11):W11503.
652 Ni C-F, Li S-G (2006) Modeling groundwater velocity uncertainty in nonstationary
653 composite porous media. Adv Water Resour 29(12):1866-1875.
654 Ni C-F, Li S-G, Liu C-J, Hsu SM (2010) Efficient conceptual framework to quantify flow
655 uncertainty in large-scale, highly nonstationary groundwater systems. J Hydrol
656 381(3-4):297-307.
657 Ni C-F, Lin C-P, Li S-G, Liu C-J, 2011. Efficient approximate spectral method to
658 delineate stochastic well capture zones in nonstationary groundwater flow systems. J.
659 Hydrol 407(1-4):184-195.
660 Oliver LD, Christakos G (1995). Diagrammatic solutions for hydraulic head moments in
661 1-D and 2-D bounded domains. Stoch Hydrol Hydraul 9(4), 269-296.

662 Pétré M-A, Rivera A, Lefebvre R (2019) Numerical modeling of a regional groundwater
663 flow system to assess groundwater storage loss, capture and sustainable exploitation
664 of the transboundary Milk River Aquifer (Canada - USA). J Hydrol 575:656-670.
665 Priestley MB (1965) Evolutionary spectra and non-stationary processes. J R Stat Soc Ser B
666 27(2):204-237.
667 Refsgaard JC (1997) Parameterisation, calibration and validation of distributed
668 hydrological models. J Hydrol 198(1-4):69-97.
669 Rodriguez-Iturbe I, Mejia JM (1974) The design of rainfall networks in time and space,
670 Water Resour Res 10(4):713-728.
671 Rotiroti M, Bonomi T, Sacchi E, McArthur JM, Stefania GA, Zanotti C, Taviani S, Patelli
672 M, Nava V, Soler M, Fumagalli L, Leoni B (2019) The effects of irrigation on
673 groundwater quality and quantity in a human-modified hydro-system: The Oglio
674 River basin, Po Plain, northern Italy. Sci Total Environ 672:342-356.
675 Rotzoll K, Gingerich SB, Jenson JW, El-Kadi AI (2013) Estimating hydraulic properties
676 from tidal attenuation in the Northern Guam Lens Aquifer, territory of Guam, USA.
677 Hydrogeol J 21(3):643-654.
678 Rubin Y, Bellin A (1994) The effects of recharge on flow nonuniformity and
679 macrodispersion. Water Resour Res 30(4):939-948.
680 Rubin Y (2003) Applied Stochastic Hydrogeology. Oxford University Press, New York,
681 N. Y.
682 Sanchez-Vila X (1997) Radially convergent flow in heterogeneous porous media. Water
683 Resour Res 33(7):1633-1641.
684 Sishodia RP, Shukla S, Graham WD, Wani SP, Jones JW, Heaney J (2017) Current and

future groundwater withdrawals: Effects, management and energy policy options for a semi-arid Indian watershed. Adv Water Resour 110:459-475.

Vanmarcke E (1983) Random Fields: Analysis and Synthesis. MIT Press, Cambridge, MA.

Vassena C, Rienzner M, Ponzini G, Giudici M, Gandolfi C, Durante C, Agostani D, (2012) Modeling water resources of a highly irrigated alluvial plain (Italy): calibrating soil and groundwater models. Hydrogeol J 20(3):449-467.

Whittle P (1954) On stationary processes in the plane. Biometrika 41:434-449.

Zamrsky D, Oude Essink GH, Bierkens MF (2018) Estimating the thickness of unconsolidated coastal aquifers along the global coastline. Earth Syst Sci Data 10(3):1591-1603.

Zhang D (2002) Stochastic Methods for Flow in Porous Media: Coping with Uncertainties. Academic Press, San Diego, C. A.

Zhou Y, Li W (2011) A review of regional groundwater flow modeling. Geosci Front 2(2):205-214.

Figure captions

Fig. 1. Dimensionless variance of depth-averaged hydraulic head in Eq. (30) versus dimensionless α-parameter for various values of dimensionless positions.

Fig. 2. Dimensionless oscillatory function in Eq. (32) versus the dimensionless wave number for various values of dimensionless α-parameter.

Fig. 3. Dimensionless cross-correlation between the ln$K$ perturbation and the perturbation

in depth-averaged head versus dimensionless α-parameter for various values of dimensionless positions.

Fig. 4. Dimensionless variance of depth-averaged hydraulic head in Eq. (30) versus dimensionless correlation scale of ln$K$ field for various values of dimensionless positions.

Fig. 5. Dimensionless mean integrated specific discharge in Eq. (42) versus dimensionless α-parameter for various values of dimensionless positions.

Fig. 6. Dimensionless variance of integrated specific discharge in the x_1-direction in Eq. (44) versus dimensionless α-parameter for various values of dimensionless positions.

Fig. 7. Dimensionless variance of integrated specific discharge in the x_2-direction in Eq. (45) versus dimensionless α-parameter for various values of dimensionless positions.

Fig. 8. (a) Variation in aquifer thickness with the best-fit estimate and (b) distribution of hydraulic conductivity as a function of distance from the aquifer outcrop in the x_1-direction.

Fig. 9. Experimental variogram of ln$K$ in the x_1-direction with the best-fit estimate (orange line).

Fig. 10. Predicted normalized mean longitudinal total discharge profiles along with two standard deviation intervals as a function of dimensionless distance.

Figures

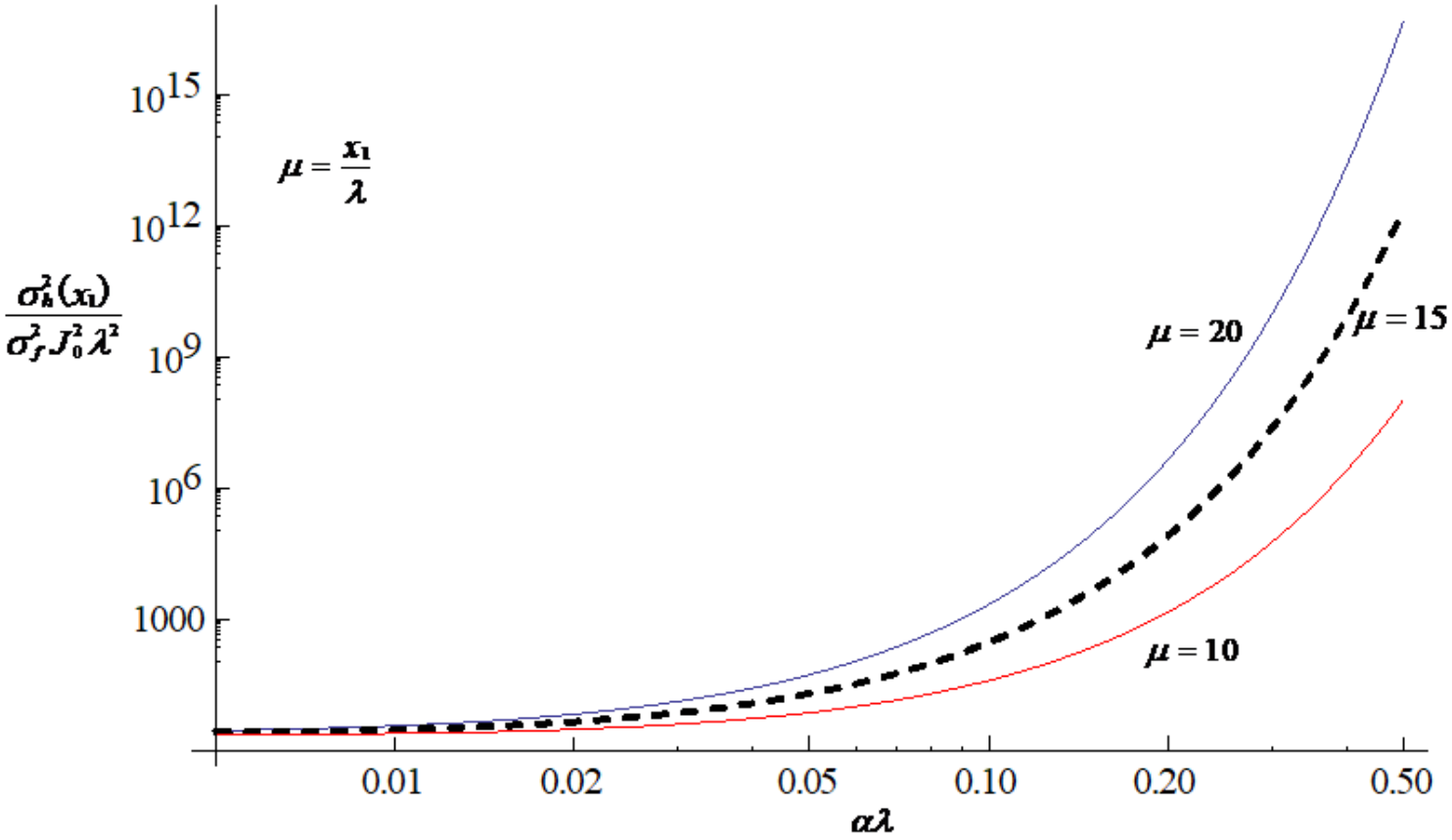

Figure 1

Dimensionless variance of depth-averaged hydraulic head in Eq. (30) versus dimensionless α-parameter for various values of dimensionless positions.

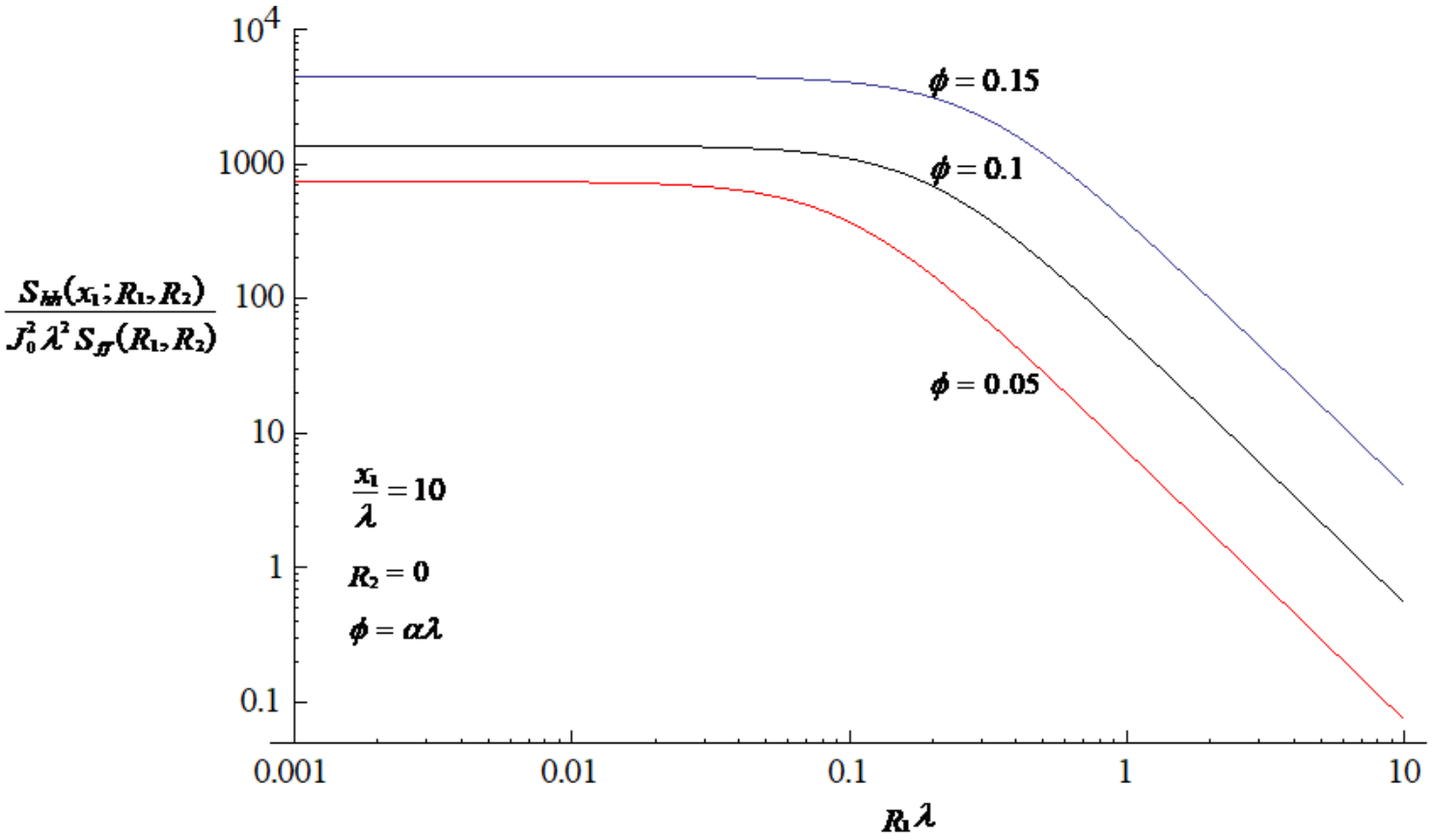

Figure 2

Dimensionless oscillatory function in Eq. (32) versus the dimensionless wave number for various values of dimensionless α-parameter.

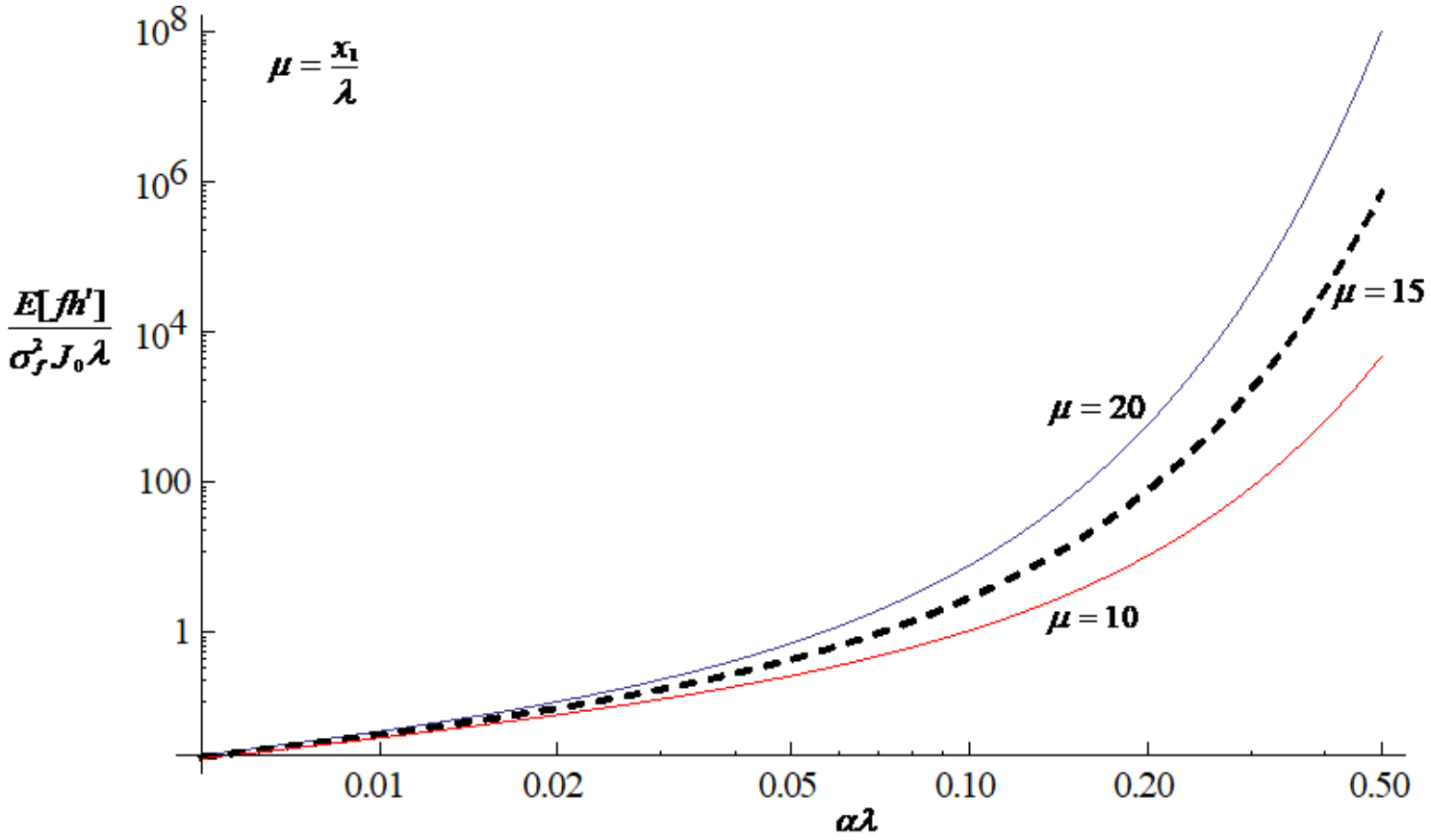

Figure 3

Dimensionless cross-correlation between the lnK perturbation and the perturbation in depth-averaged head versus dimensionless α-parameter for various values of dimensionless positions.

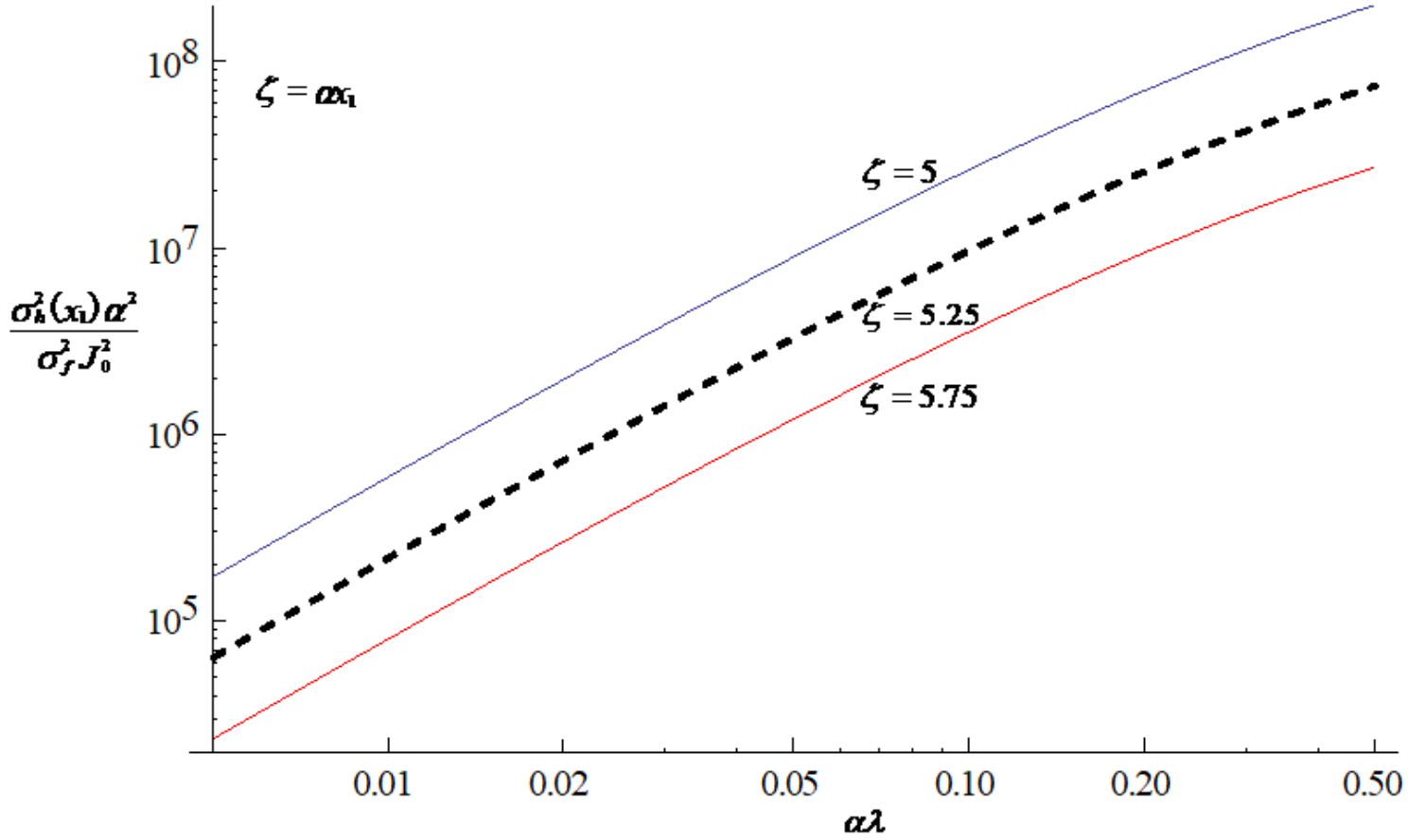

Figure 4

Dimensionless variance of depth-averaged hydraulic head in Eq. (30) versus dimensionless correlation scale of lnK field for various values of dimensionless positions.

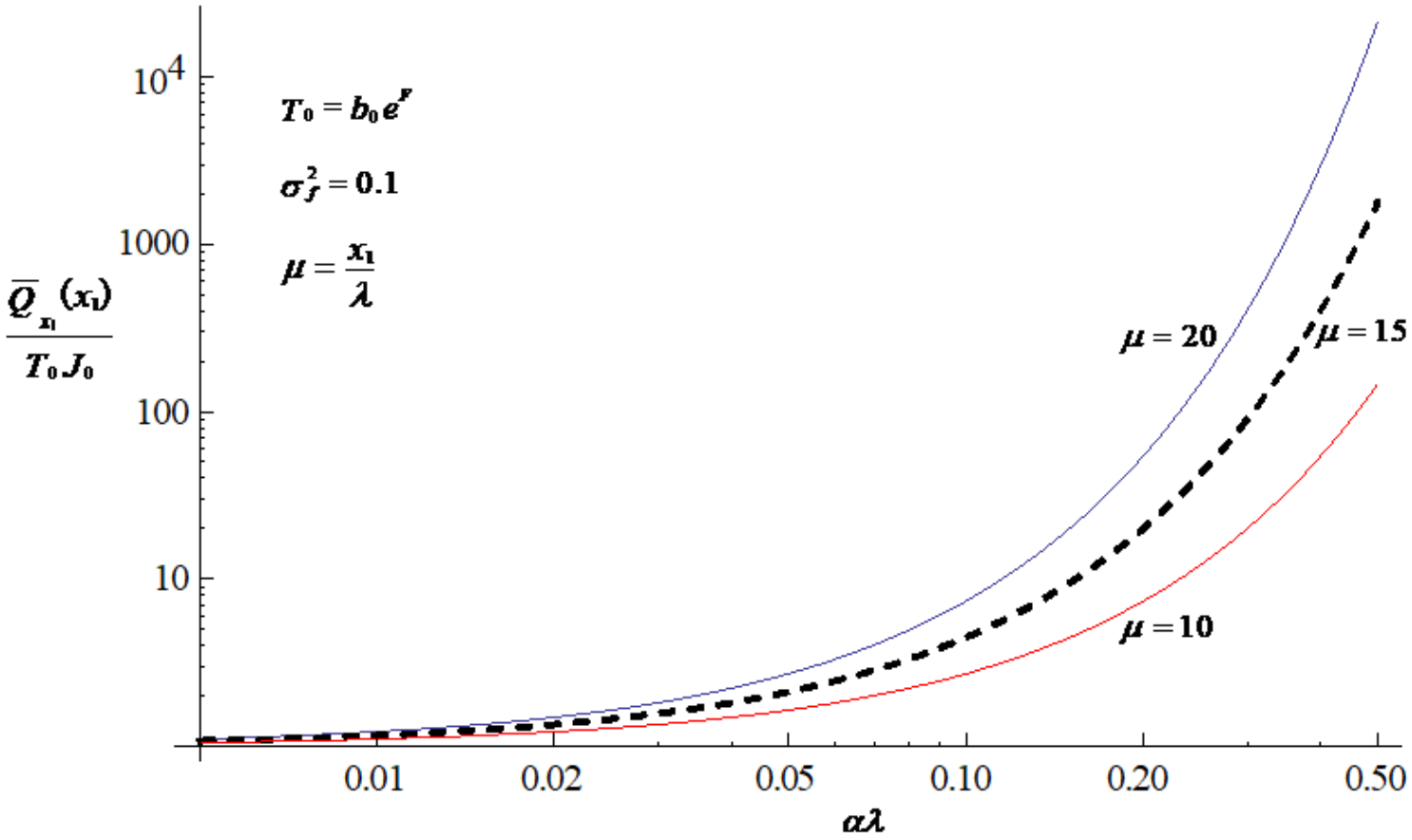

Figure 5

Dimensionless mean integrated specific discharge in Eq. (42) versus dimensionless α-parameter for various values of dimensionless positions.

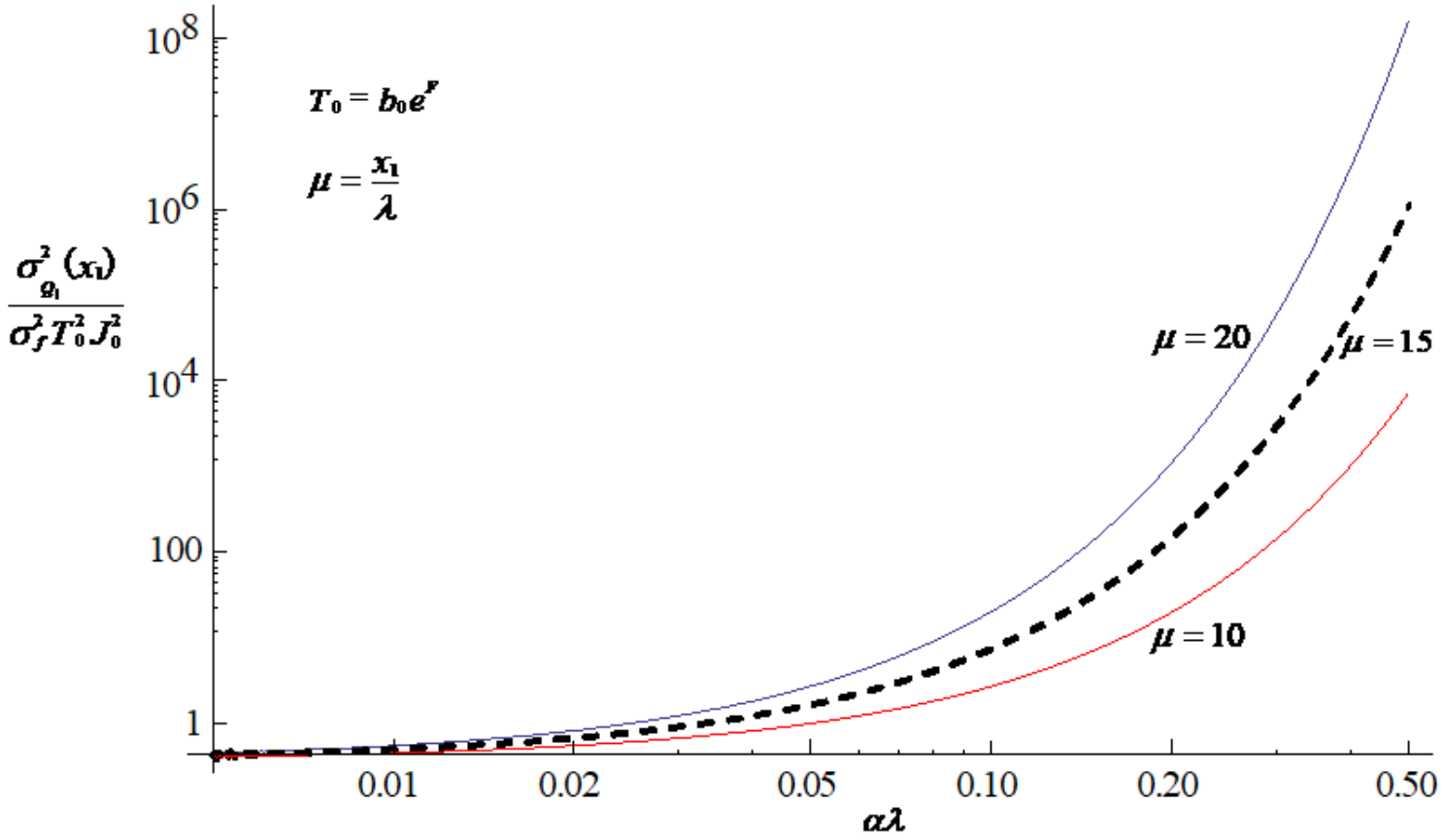

Figure 6

Dimensionless variance of integrated specific discharge in the x1-direction in Eq. (44) versus dimensionless α-parameter for various values of dimensionless positions.

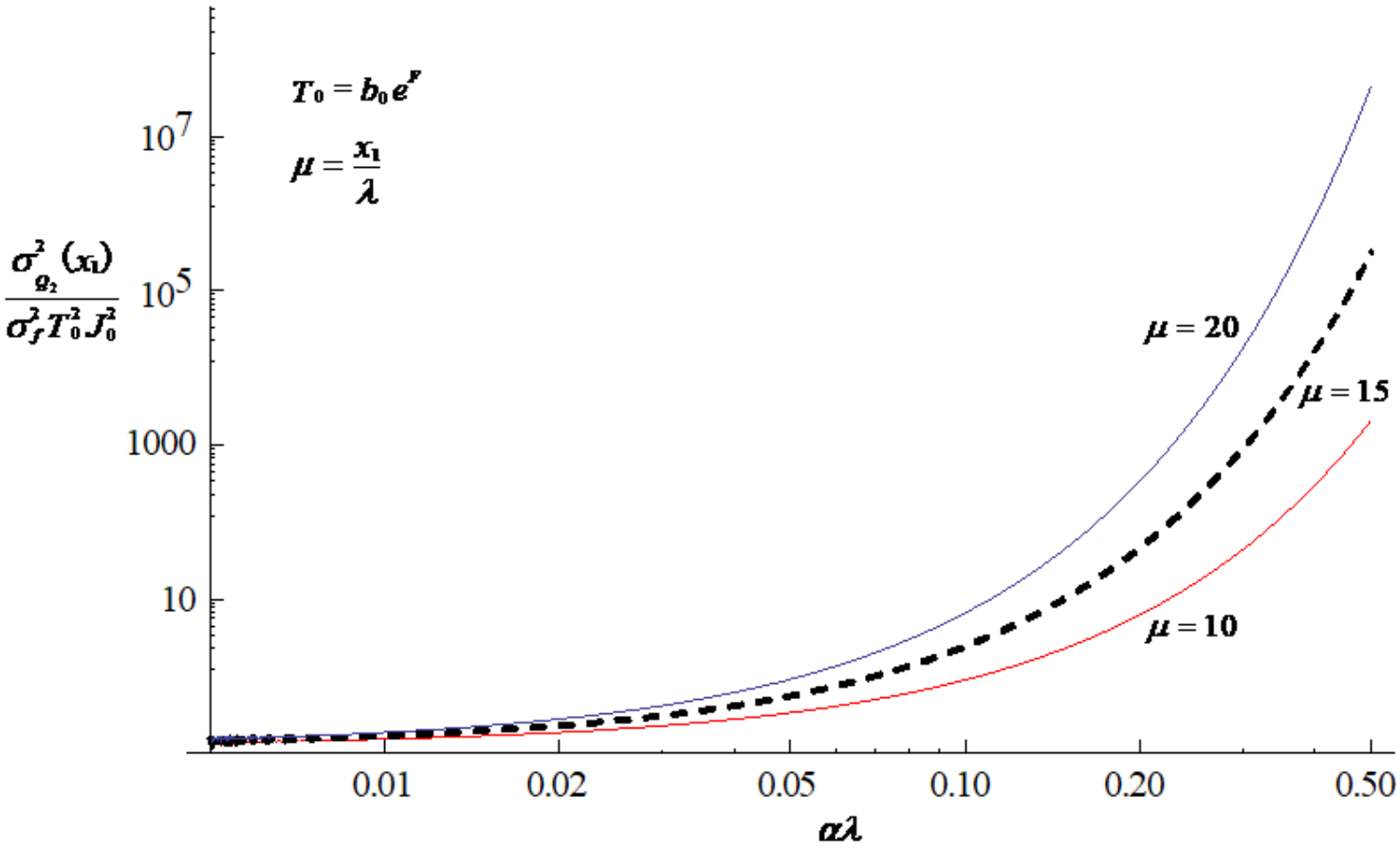

Figure 7

Dimensionless variance of integrated specific discharge in the x2-direction in Eq. (45) versus dimensionless α-parameter for various values of dimensionless positions.

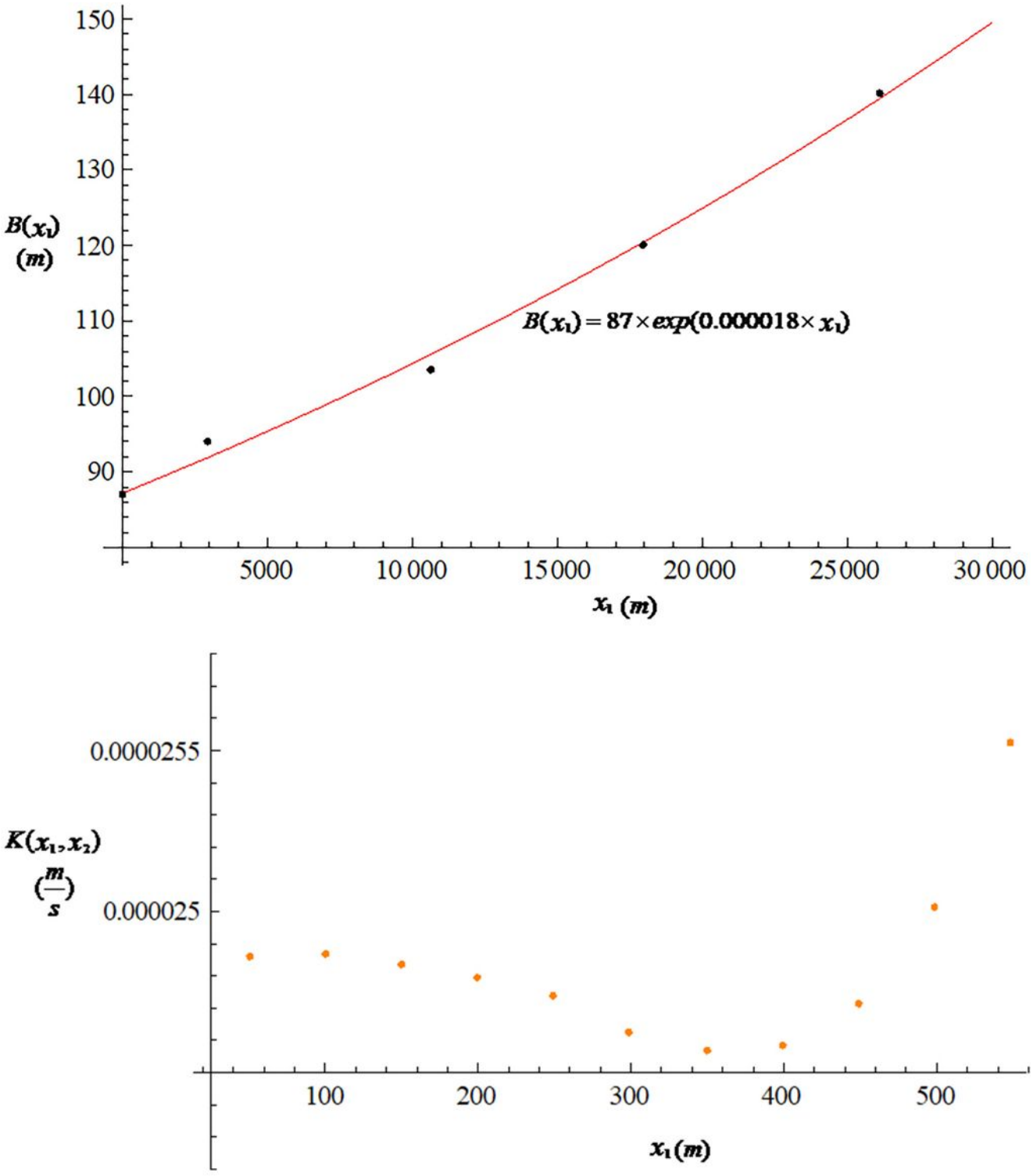

Figure 8

(a) Variation in aquifer thickness with the best-fit estimate and (b) distribution of hydraulic conductivity as a function of distance from the aquifer outcrop in the x1-direction.

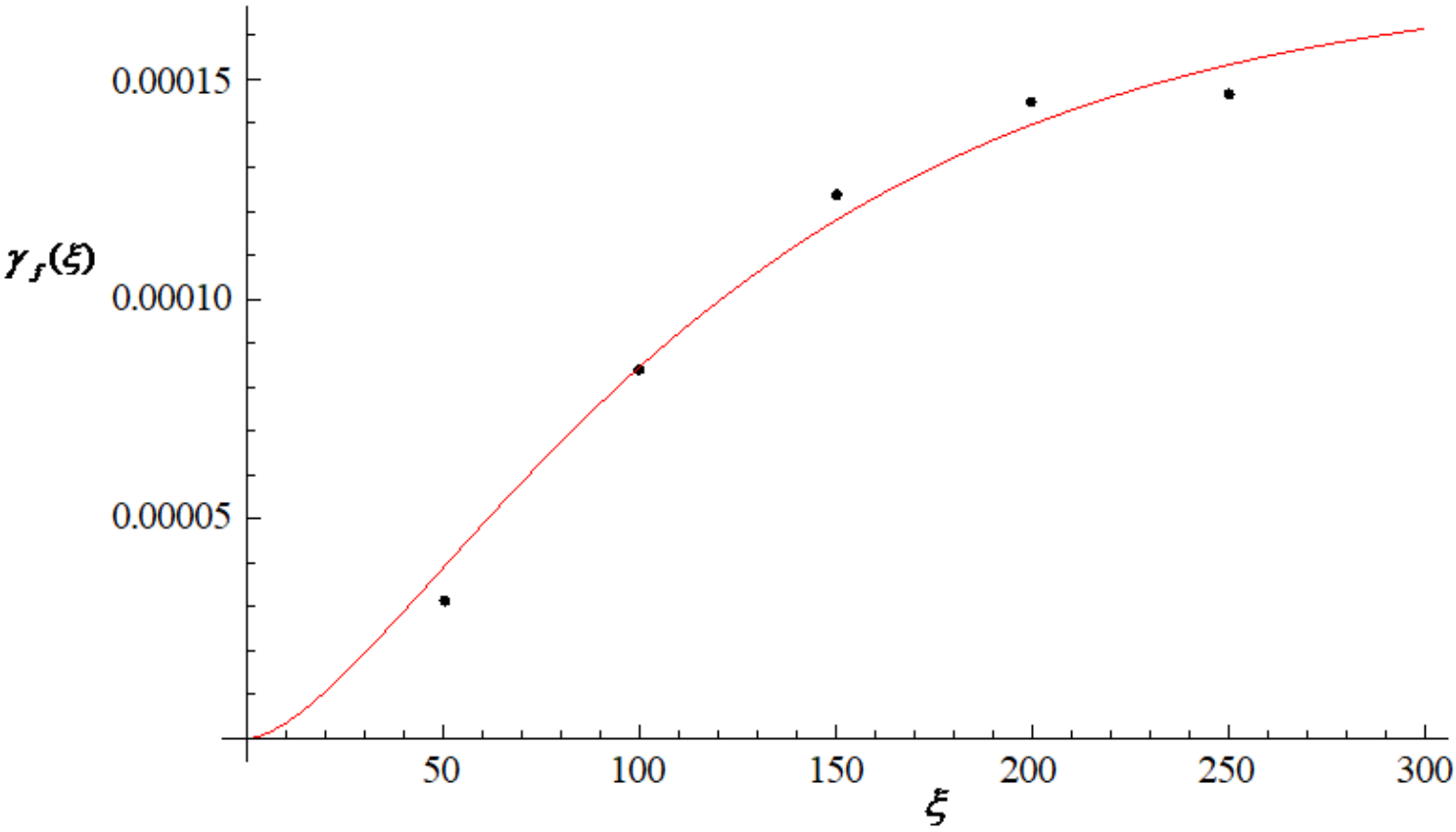

Figure 9

Experimental variogram of lnK in the x1-direction with the best-fit estimate (orange line).

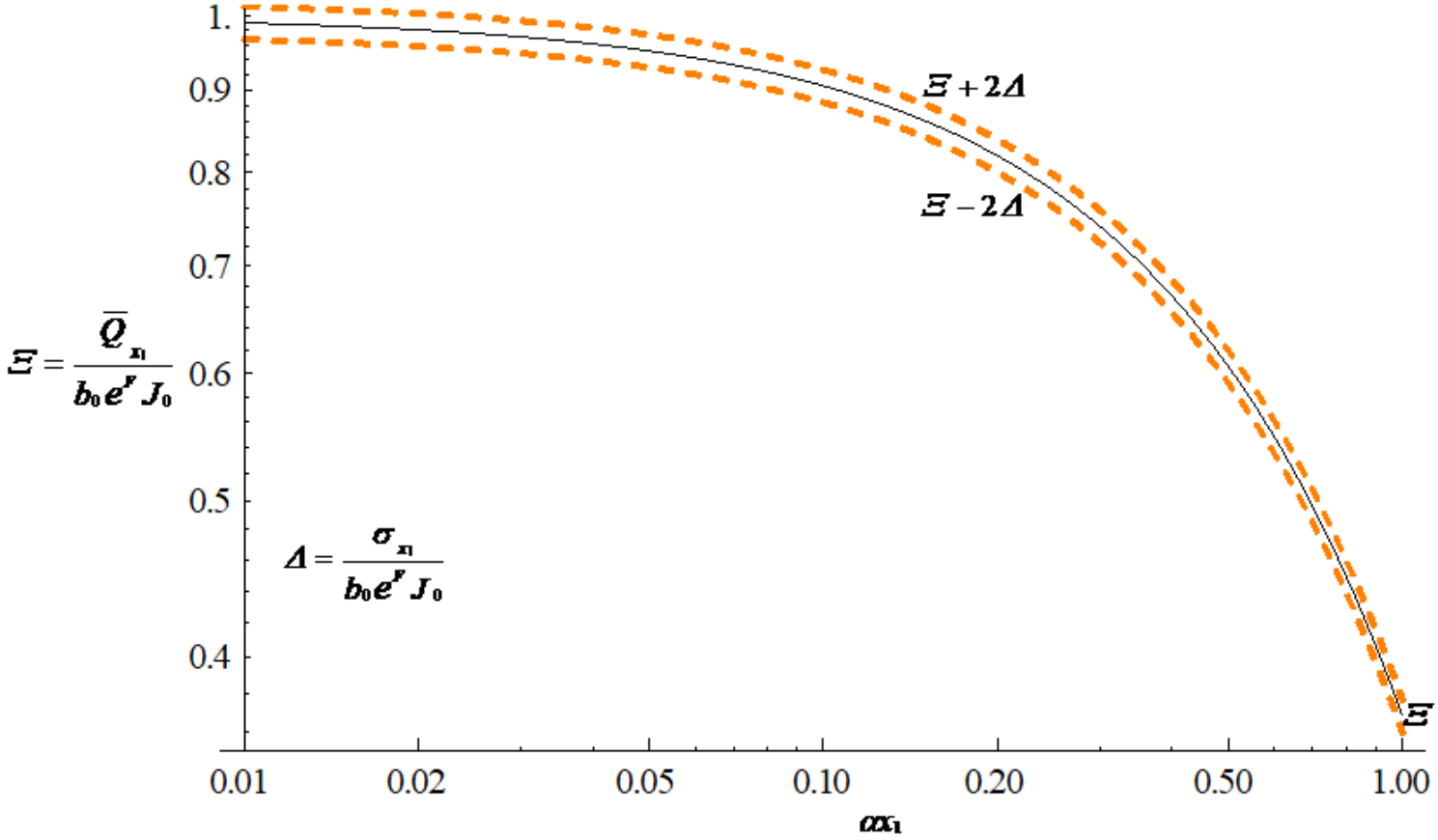

Figure 10

Predicted normalized mean longitudinal total discharge profiles along with two standard deviation intervals as a function of dimensionless distance.